Neural Network-based Robust Linearization and Compensation Technique for Sensors under Nonlinear Environmental Influences

Jagdish C. Patra, *Member IEEE*, Goutam Chakraborty, *Senior Member IEEE* and Pramod K. Meher, *Senior Member, IEEE*

***Abstract*— A novel artificial neural network (NN)-based technique is proposed for enabling smart sensors to operate in harsh environments. The NN-based sensor model automatically linearizes and compensates for the adverse effects arising due to nonlinear response characteristics and nonlinear dependency of the sensor characteristics on the environmental variables. To show the potential of the proposed NN-based technique, we have provided results of a smart capacitive pressure sensor (CPS) operating under a wide range of temperature variation. A multilayer perceptron is utilized to transfer the nonlinear CPS characteristics at any operating temperature to a linearized response characteristics. Through extensive simulated experiments, we have shown that the NN-based CPS model can provide pressure readout with a maximum full-scale error of only $\pm 1.5\%$ over a temperature range of -50 to 200^0C with excellent linearized response for all the three forms of nonlinear dependencies considered. Performance of the proposed technique is compared with a recently proposed computationally efficient NN-based extreme learning machine (ELM). The proposed MLP-based model is tested by using experimentally measured real sensor data, and found to have satisfactory performance.**

Keywords
Intelligent and smart sensors, artificial neural networks, pressure sensor, linearization, auto-compensation, harsh environment.

I. INTRODUCTION

Sensors are widely used in industrial processes, automobiles, robotics, avionics and other systems to monitor and control the system behavior. Besides, the use of precise, accurate and low power sensors has recently emerged in many sensor network applications. Capacitive sensors, because of their high sensitivity and low power consumption, are extensively used in various applications to measure pressure, force, position, speed, acceleration, liquid level, dielectric properties and flow of materials. However, some of the drawbacks of capacitive sensors are that: (i) the change in capacitance of the sensor due to applied pressure is small compared to the offset capacitance and (ii) their response characteristics are highly nonlinear.

Another problem associated, in general, with all sensors is that, their response characteristics are influenced by the disturbing environmental parameters, e.g., temperature, humidity and pollution. For example, in case of a capacitive pressure sensor (CPS), its response depends not only on the applied pressure but also on the environmental temperature. This problem becomes severe, especially when the capacitive sensor is operated in a harsh environment where temperature variation is large.

Usually, an exact mathematical model of a sensor showing the relationship between the measurand and its response, and the dependency of sensor output on environmental parameters, is not available. Further, since most of the sensors exhibit some amount of nonlinear response characteristics, and the environmental parameters influence the sensor behavior nonlinearly, the problem of obtaining an accurate readout and its calibration becomes highly complex. Some of the ideal properties of a sensor include linear response characteristics, auto-correction for the adverse effects of nonlinear environmental parameters, high sensitivity and accuracy, and low power consumption. However, in practical situations, it is not easy to achieve ideal sensor characteristics, especially when the sensor is operating in a harsh environment.

In order to obtain an accurate and precise readout from a CPS the adverse effects of the environmental parameters and nonlinear characteristics are required to be suitably compensated. In this direction, for compensation of offset capacitance, temperature and auto-calibration, switched capacitor-based techniques [1], [2], and ROM and over-sampling delta-sigma demodulation techniques [3], [4] have been reported. Some of the digital signal processing-based techniques, both iterative and non-iterative, for pressure sensor linearization and compensation are found in [5]-[7]. To reduce the computational load, a non-iterative 2-dimensional calibration and linearization technique [8] and a microcontroller-unit (MCU)-based self-calibration technique [9] have been reported. Two analog linearization methods for capacitive pressure sensors have also been proposed [10]. The first method uses the feedback from output to control the excitation voltage while the second method uses a push-pull capacitive structure, in which a pair of pressure-sensitive capacitors operate in a push-pull configuration. An FPGA-based adaptive thermal compensation of strain gauge sensors is reported in [11], in which it is shown

J. C. Patra is with the School of Computer Engineering, Nanyang Technological University, Singapore 639798; e.mail: aspatra@ntu.edu.sg. A part of this work was carried out while he visited Iwate Prefectural University, Japan, under the Tan Chin Tuan Fellowship Program during December 2005.

G Chakraborty is with the Department of Software and Information Science, Iwate Prefectural University, Takizawa, Japan 020-0193; e.mail goutam@soft.iwate-pu.ac.jp.

P. K. Meher is with the School of Computer Engineering, Nanyang Technological University, Singapore 639798; e.mail: aspkmeher@ntu.edu.sg.

that Newton's algorithm is more suitable for offset compensation in shock measurement. A self-calibration and linearization algorithm for smart sensor applications based on a progressive polynomial method and an optimal choice of calibration points have been suggested in [12]. These techniques provide limited solutions to the complex problem under the assumptions that the range of variations of environmental parameters are small and the influence of environmental parameters on the sensor characteristics is linear.

Recently, artificial neural networks (NNs) have emerged as a powerful learning technique to perform complex tasks in dynamic and nonlinear environments. These networks are endowed with unique capability of universal approximation and the ability to learn from and to adapt according to their environment. Another important property of the NNs is their fault-tolerance capability, which allows graceful degradation of performance when the network is partially damaged. Because of these characteristics numerous successful applications of NNs are found in various fields of science, engineering and industry [13], including instrumentation and measurement [14], [15].

It is shown that the NN-based approximations for measurement data perform much better than those of classical methods of data interpolation and least mean square regression [16]-[18]. Application of NNs with superior performance in compensation for environmental dependency and nonlinearities of sensor characteristics of pressure sensors [19]-[21], magnetic field measurement [22] and ultrasonic distance measurement [23], have been reported. An NN-based technique to compensate for the nonlinear interference of structural and geometrical parameters in a differential eddy-current displacement transducer with satisfactory results has been reported [24]. An NN-based fault detection scheme for Wheatstone bridge transducer [25] and NN-based compensation scheme for disturbing parameters in a strain gauge transducer by taking a small range of disturbances have been reported [26].

In some of the earlier reported works [19]-[21], we have shown the effectiveness of NNs in auto-calibration and compensation for adverse effects of linear and nonlinear influences of disturbing parameters. We have shown that the NN-based models are quite effective and capable to provide accurate readout when the sensor operates in a harsh environment with wide variation of surrounding temperature. However, in these NN-based techniques, the main emphasis was to fit the nonlinear response characteristics data most accurately even if the sensor characteristics changes under the influence (linear or nonlinear) of the disturbing parameters (e.g., temperature). These works were concentrated in finding a neural model to obtain the sensor response accurately under the influence of linear or nonlinear disturbing parameters. The important issue of linearization was not considered in those papers.

Typical response characteristics of a CPS operating at different temperatures is shown by the upper five curves in Fig. 1. The middle curve (solid line) represents the sensor characteristics at normal temperature of 25^0C. Due to nonlinear influence of the disturbing parameter (in this case, the temperature) the sensor characteristics change drastically from the normal operating temperature of 25^0C. It is always

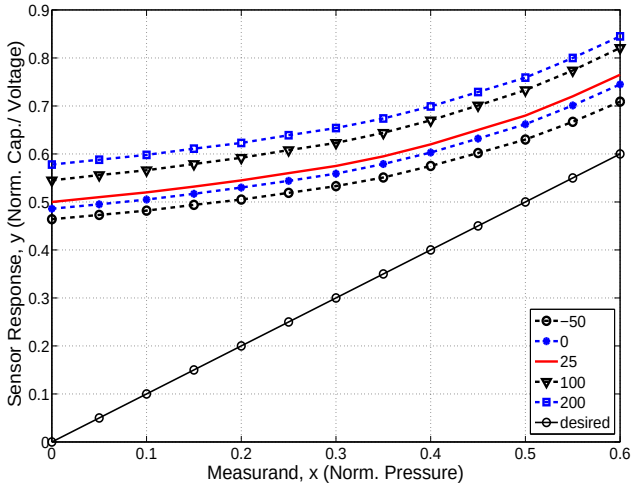

Fig. 1. The concept of linearization for a sensor.

desirable to have linear response characteristics for a sensor/ transducer. It makes the measurement and calibration quite simple. It implies that the sensor/ transducer response can be given by $y = mx + c$, where y is the transducer response (e.g., voltage or current), x is the measurement variable (e.g., pressure), m is the slope (sensor gain) and c is a constant. A true linear characteristics is obtained when $m = 1$ and $c = 0$ (the bottom straight line in Fig. 1). In the case of a sensor, a true linear characteristics is most desirable, as it makes calibration, validation and fault detection quite easy and consequently a correct readout becomes quite simple.

However, obtaining a true linear characteristics is not an easy task. It becomes more complex when the disturbing parameters (e.g., temperature) influence the sensor characteristics nonlinearly. In this direction, a linearization technique using a simple multilayer perceptron (MLP) for a temperature sensor (a negative temperature coefficient resistor) has been reported [27]. Here, a linearization of 0.5% was obtained, but only for a small operating range of 60^0C. Besides, the effect of disturbing environmental parameters were not considered. In our earlier papers [19]-[21] the emphasis was to employ the NNs to estimate the sensor's nonlinear response characteristics accurately (upper curves in Fig. 1). However, in the current paper the focus is to use the NN to obtain an exact linear response characteristics for a sensor (the bottom solid straight line in Fig. 1).

In this paper, we present a novel NN-based technique to develop an intelligent pressure sensor that can provide true linear response characteristics. Here, we have shown that the proposed NN-based CPS sensor model can provide a true linear response characteristics even if the CPS is operated in a harsh environment with a wide variation of temperature ranging from -50 to 200^0C. In addition, we have assumed that the CPS response characteristics are nonlinearly influenced by the environmental temperature. The proposed MLP model achieves the true linear response characteristics (as shown in Fig. 1) which is independent of the nonlinear sensor characteristics and its nonlinear dependency on the environmental temperature. Through extensive computer simulations,

we have shown that the maximum full-scale (FS) error remains within $\pm 1.5\%$ under wide possible operating conditions, by using three forms of nonlinear dependencies.

The rest of the paper is arranged as follows. Section II presents a brief theoretical background of the CPS and the switched capacitor interface. Section III provides details of the proposed MLP-based sensor modeling scheme. Brief description of a recently proposed NN, the extreme learning machine, is provided in Section IV. Extensive simulated experiments are detailed in Section V. Section VI provides the performance evaluation and discussions on the results of the experiments. Performance comparison between the MLP- and extreme learning machine-based sensor linearization schemes is also made in this section. The details of an experimental setup to measure data from a force sensor and the performance results of the proposed MLP-based model with these data are provided in Section VII. Finally, conclusions of the present study are summarized in Section VIII.

II. CAPACITIVE PRESSURE SENSOR AND SWITCHED CAPACITOR INTERFACE

A capacitive pressure sensor (CPS) senses the applied pressure in the form of elastic deflection of its diaphragm. The capacitance of the CPS resulting from the applied pressure P at the ambient temperature T is given by [3]:

$$C(P,T) = C_0(T) + \Delta C(P,T), \tag{1}$$

where $\Delta C(P,T)$ is the change in capacitance and $C_0(T)$ is the offset capacitance, *i.e.*, the zero-pressure capacitance, at the ambient temperature T. The above capacitance may be expressed in terms of capacitances at the reference temperature, T_0 as:

$$C(P,T) = C_0(T_0)f_1(T) + \Delta C(P,T_0)f_2(T), \tag{2}$$

where, $C_0(T_0)$ is the offset capacitance and $\Delta C(P,T_0)$ is the change in capacitance, at the reference temperature, T_0. The nonlinear functions, $f_1(T)$ and $f_2(T)$, determine the effect of temperature on the sensor characteristics [3]. This model provides sufficient accuracy in determining the influence of temperature on the sensor response characteristics.

The capacitance change in the CPS due to applied pressure at the reference temperature T_0 is given by [3],[4]:

$$\Delta C(P,T_0) = C_0(T_0)P_N\frac{1-\tau}{1-P_N}, \tag{3}$$

where τ is the sensitivity parameter, P_N is the normalized applied pressure given by $P_N = P/P_{max}$, and P_{max} is the maximum permissible applied pressure. The parameters τ and P_{max} depend on the geometrical structure and physical dimensions of the CPS. Since $\Delta C(P,T_0)$ becomes very large as P_N approaches 1, in practice, the value of P_N is normally kept within 0.9.

In this study, in conformance with practical conditions, we have considered that the ambient temperature nonlinearly influences the CPS characteristics. In order to study the nonlinear dependence of ambient temperature, we assumed that the capacitance change in a CPS is influenced by a nonlinear function which is a third order polynomial of normalized temperature. The nonlinear dependency functions $f_i(T),\ i = 1$ and 2 may be expressed as:

$$f_i(T) = 1 + g_i(T), \tag{4}$$

where

$$g_i(T) = \kappa_{i1}T_N + \kappa_{i2}T_N^2 + \kappa_{i3}T_N^3, \tag{5}$$

and the normalized temperature, T_N is given by $T_N = (T - T_0)/(T_{max} - T_{min})$. The maximum and the minimum operating temperatures are denoted by T_{max} and T_{min}, respectively. The coefficients κ_{ij}, where $i = 1$ and 2, and $j = 1, 2,$ and 3, determine the extent of nonlinear influence of the temperature on the sensor characteristics. Note that when $\kappa_{ij} = 0$ for $j = 2$ and 3, the influence of the temperature on the CPS response characteristics becomes linear.

The normalized capacitance at any temperature T may be expressed as:

$$C_N = C(P,T)/C_0(T_0). \tag{6}$$

This may be expressed using Eqns. (2) and (3) as:

$$C_N = f_1(T) + \gamma f_2(T), \tag{7}$$

where $\gamma = P_N(1-\tau)/(1-P_N)$. Because of the requirement of the proposed NN modeling, C_N in (7) is divided by a scale factor (SF) of 2, so as to limit its value within 1. The value of γ becomes zero when the applied pressure is zero. Therefore, the normalized zero-pressure capacitance, *i.e.*, the normalized offset capacitance at any temperature T, is given by:

$$C_{N0} = f_1(T) = 1 + g_1(T). \tag{8}$$

By choosing appropriate values of κ_{ij} and using (2)-(7), one can simulate the CPS characteristics that is nonlinearly influenced by the ambient temperature.

A switched capacitor interface (SCI) for the CPS is shown in Fig. 2, where the CPS is represented by $C(P)$. The SCI output provides a voltage signal proportional to the capacitance change in the CPS due to the applied pressure. The SCI operation can be controlled by a reset signal θ. When $\bar{\theta} = 1$ (logic 1), $C(P)$ charges to the reference voltage V_R while the capacitor C_S is discharged to ground. On the other hand, when $\theta = 1$, the total charge $C(P)V_R$ stored in $C(P)$ is transferred to C_S producing an output voltage given by:

$$V_O = K \cdot C(P), \tag{9}$$

where $K = V_R/C_S$. It may be noted that if the ambient temperature changes, then the SCI output also changes, although the applied pressure remains the same. By choosing proper values of C_S and V_R, the normalized SCI output V_N may be obtained in such a way that

$$V_N = C_N. \tag{10}$$

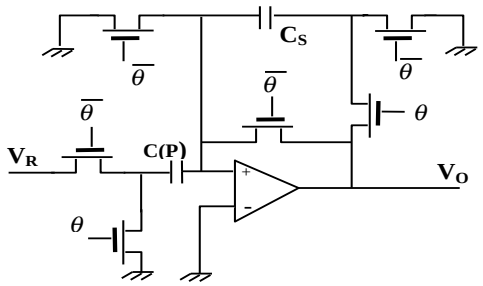

Fig. 2. The switched capacitor interface circuit along with capacitive pressure sensor.

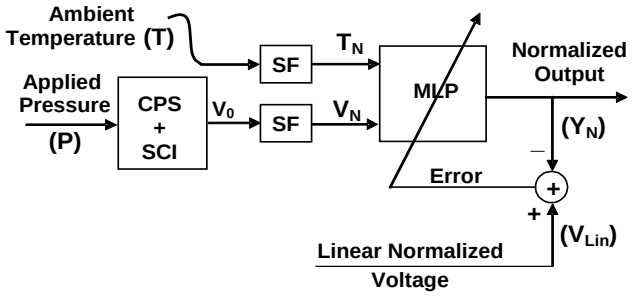

Fig. 3. An MLP-based scheme for a capacitive pressure sensor to transfer the response characteristics at any temperature to linear response characteristics.

III. THE MLP-BASED CPS MODEL

The proposed MLP-based model uses an MLP for automatic calibration and compensation for nonlinear temperature dependency of the ambient temperature on the sensor characteristics. In addition, it is trained to provide a linear response characteristics. We know that the sensor characteristics of a CPS is nonlinear and varies with the environmental temperature. Further, the environmental temperature influences the response characteristics in a highly nonlinear manner. The objective here is to obtain a linear characteristics for the sensor that is independent of its nonlinear characteristics and its nonlinear dependency on environmental temperature.

In order to achieve this objective we utilize an MLP to transfer the nonlinear sensor characteristics at any temperature (the upper curves in Fig. 1) to a linear normalized sensor characteristics (lower straight line in Fig. 1). Therefore, when the surrounding environmental temperature changes, although the nonlinear sensor characteristics change in a complex manner due to the nonlinear temperature dependency, the proposed MLP-based CPS model will always provide a linearized response.

In the proposed MLP-based CPS model, all the signals are suitably scaled by appropriate SFs to keep their range within ± 1.0. The model operates in two phases: the training phase and the test phase. In the training phase, the NN is trained to learn the sensor characteristics and environmental dependency. Several known datasets are needed to train the MLP. An input pattern, and its corresponding target (also called the desired) pattern constitute one pair of data in the dataset. The total available datasets are segregated into two parts. The first part, called training set, is used for training of the NNs, and the other part called test set, is used to test the model for unseen inputs to verify the effectiveness of the technique.

During the training phase, an input pattern from the training set is applied to the NN and its output is computed. Then the output is compared with the corresponding target pattern. The error generated out of this comparison is used thereafter to update the weights of the MLP by using the most popular backpropagation (BP) algorithm [13]. This training procedure continues until the error reaches a preset minimum value. Next, the final weights are stored in an EEPROM. These weights are used during testing and actual use of the sensor model.

In the second phase, the test phase, the stored final weights are loaded into the MLP. An input pattern from the test set is applied to the NN model and its output is computed. If the NN output and the target pattern match closely, then it may be said that the NN model has learnt the sensor characteristics satisfactorily.

To illustrate the effectiveness of the model for nonlinear dependency of sensor characteristics on temperature, we have chosen three forms of nonlinear functions denoted by $NL1$, $NL2$ and $NL3$. A linear function denoted by $NL0$ is also used for comparison purpose. These nonlinear functions are generated by different sets of coefficients κ_{ij} in (5). In this study, the temperature information is assumed to be available. It can be obtained by using another temperature sensor. As the sensor characteristics do not change drastically with a small variation of temperature, the temperature sensor need not be of high accuracy.

In the first stage, the MLP is trained to learn to transfer the sensor characteristics at any temperature to the normalized linearized response characteristics. The scheme for this is shown in Fig. 3. Here, the inputs to the MLP consist of the normalized temperature T_N and the normalized SCI output V_N (10). The normalized SCI output refers to the capacitive pressure transducer output which determines the pressure readout. For a true linear response characteristics, the SCI output should be linearly proportional to the normalized applied pressure. Therefore, we choose the target output $V_{Lin} = mP_N$. During the training phase the MLP attempts to produce an output which is a good estimate of the target output. By changing the value of the gain parameter m we can obtain the linearized sensor characteristics with a different gain.

One dataset for a specific temperature is obtained by recording the SCI output (V_N) for different values of applied pressure at that temperature. Next, at different temperature values, covering the full operating range, several datasets are generated. The MLP is trained by taking the patterns from the training set, and its weights are updated by using the BP algorithm. After completion of the training, the MLP weights are frozen and stored in an EEPROM.

In the present study, we have used an MLP with BP algorithm for the sensor linearization application, because, the MLP is robust and a time-proven NN architecture. However, the major drawback of MLP is its large training time and slow convergence. Therefore, it may not be suitable for online applications. However, our main purpose in this study is to highlight successful application of an NN to the complex problem of sensor linearization and compensation. There

are several other NN architectures, e.g., radial-basis function (RBF) networks, support vector machines (SVM), Bayesian networks, which may, however, be used for this application. In the next Section, we briefly describe a computationally efficient emerging NN architecture, extreme learning machine (ELM). We used the ELM for the CPS linearization problem and compared its performance with the MLP.

IV. EXTREME LEARNING MACHINE

The extreme learning machine is recently proposed by Huang et al. [28]-[31]. It is a control-parameter-free powerful supervised learning architecture and is capable of very fast learning. Moreover, it has low computational complexity. Therefore, it may be conveniently used for on-line applications. It is a two layer feedforward fully-connected neural network in which the first layer weights and bias values are selected randomly and independently from the training dataset. During training phase, the weighted sum of the input pattern is passed through the hidden layer nodes with a piecewise continuous sigmoid nonlinearity. The output layer weight matrix and the bias vector are directly obtained by using pseudo-inverse technique from the output of the hidden layer and the desired output. Huang et al. [28]-[31] have shown that the ELM can be an universal approximator. More details of ELM and mathematical treatment on ELM may be found in [28]-[31]. We have applied ELM for the CPS sensor linearization problem. Its performance comparison with the MLP-based model is carried out in Section VI.

V. SIMULATION STUDIES

We carried out extensive simulation studies for performance evaluation of the proposed MLP-based CPS model. In the following, we describe the details of the simulation study.

A. Preparation of Datasets

All the parameters of the CPS, such as the ambient temperature, the applied pressure, and the SCI output voltage, used in the simulation study were suitably normalized to keep their values within ± 1.0. Appropriate SFs were chosen for this purpose. The datasets needed for training and testing of the NN were generated as follows. The SCI output voltage (V_N) was recorded at the reference temperature ($T_0 = 25^0C$) with different known values of normalized pressure (P_N) chosen between 0.0 and 0.6 at an interval of 0.05. These 13 pairs of data (P_N versus V_N) constitute one dataset at the reference temperature.

To study the influence of temperature on the CPS characteristics, three forms of nonlinear functions $NL1$, $NL2$, and $NL3$, and a linear form $NL0$ were generated, by using (4) and (5). We selected values of the κ_{ij} arbitrarily and tabulated in Table I. Using these values, we observed that the dependency functions introduce a large amount of nonlinearity in the sensor response characteristics.

Next, with the knowledge of the dataset at the reference temperature and the chosen values of κ_{ij}, the response characteristics of the CPS for a specific ambient temperature were generated using (7). The response characteristics consist of 13 pairs of data (P_N and V_N) and correspond to a dataset at that temperature. For a temperature range from -50^0C to 200^0C, at an increment of 10^0C, twenty-six such datasets, each containing 13 data pairs, were generated. Next, these datasets were divided into two groups: the training set and the test set. The training set, used for training the NNs, consists of five datasets corresponding to -50, 10, 70, 130 and 190^0C, and the remaining twenty one datasets were used as the test set. To illustrate the nature of the nonlinear forms of temperature dependency, variation of the normalized capacitance (at $P_N = 0.3$) with temperature for $NL0$, $NL1$, $NL2$ and $NL3$ are plotted in Fig. 4. Note that even though there is no change in applied pressure, the sensor's normalized capacitance C_N (and as such the SCI output V_N) changes nonlinearly with temperature. We believe that the above selected values of κ_{ij} (see Table I) provide adequate nonlinear influence of temperature on the CPS characteristics and its complexity is similar to that of practical situations. This is evident from Fig. 4.

The sensor response characteristics at different temperatures for the four forms of dependencies and the desired linear response are plotted in Fig. 5. It can be seen that the response characteristics of the sensor change nonlinearly over the temperature range. Besides, the change in response characteristics differs substantially for different forms of nonlinear dependencies. However, it is important to note that, the sensor's linear response characteristics should remain the same in spite of different nonlinear temperature dependencies and the changes

TABLE I

THE VALUES OF κ_{ij} FOR THE LINEAR AND NONLINEAR FORMS OF TEMPERATURE DEPENDENCIES.

NL form	κ_{11}	κ_{12}	κ_{13}	κ_{21}	κ_{22}	κ_{23}
$NL0$	0.10	0.00	0.00	0.20	0.00	0.00
$NL1$	0.25	-0.25	0.10	0.20	-0.40	0.40
$NL2$	0.30	0.10	-0.30	0.20	-0.20	-0.10
$NL3$	0.40	-0.15	-0.15	0.25	0.30	-0.60

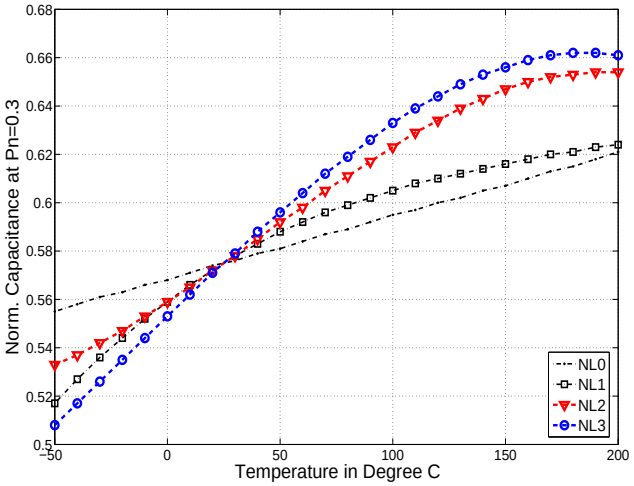

Fig. 4. Variation of normalized capacitance (C_N at $P_N = 0.3$) with temperature for the linear and three nonlinear forms of temperature dependencies ($NL0$, $NL1$, $NL2$ and $NL3$). The value of C_N changes nonlinearly with temperature even though P_N is fixed at 0.3.

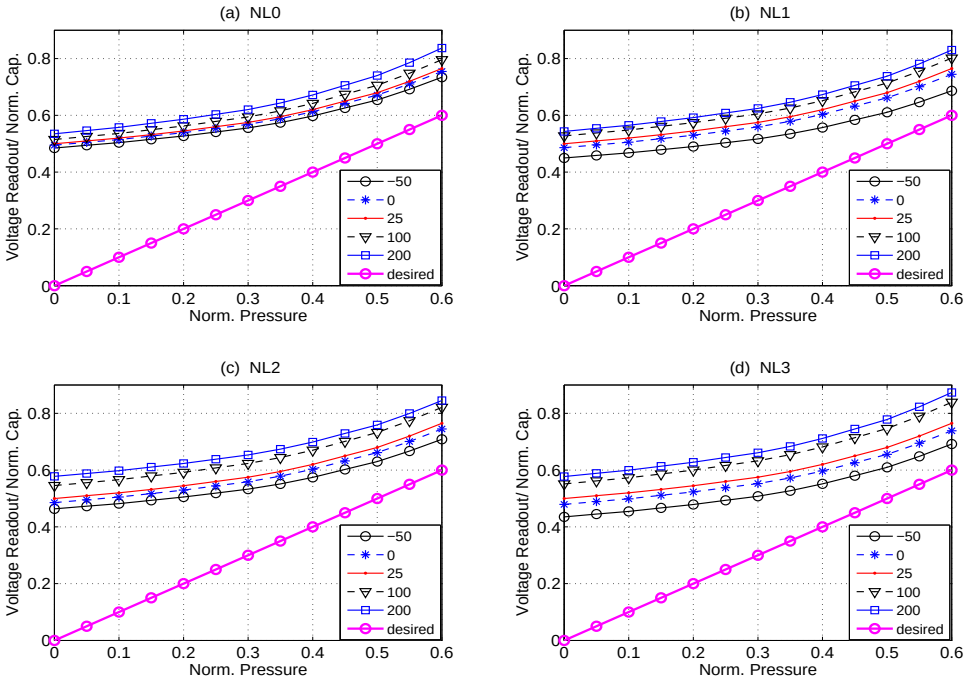

Fig. 5. The desired linear characteristics and the actual SCI output (the CPS response characteristics) while the CPS is operating at different temperatures (-50, 0, 25, 100 and 200^0C) under a linear and three forms of nonlinear dependencies. (a) $NL0$; (b) $NL1$; (c) $NL2$; (d) $NL3$.

in ambient temperature.

B. Training and Testing of MLP

A 2-layer MLP with $\{2-5-1\}$ architecture was chosen in this modeling problem (see Fig. 3). The number of nodes including the bias units in the input, hidden and the output layers are 3, 6 and 1, respectively. Thus, the MLP contains only 21 weights. Each node of the hidden layer and the output layer consists of a bipolar sigmoid nonlinear function. The two inputs to the MLP were the normalized temperature (T_N) and the normalized SCI output voltage (V_N). The linear normalized voltage V_{Lin} was used as the target output for the MLP.

Initially, all the weights of the MLP were set to random values within ± 0.5. During training, the five datasets were chosen randomly. Also, the individual patterns of each set were selected in a random manner. After application of one input pattern, the MLP produces an output. The output value was compared with the target output to obtain an error value. This error was then used to update the weights of the MLP using the BP algorithm. The learning parameter α and the momentum factor β (used in the BP algorithm) were selected as 0.3 and 0.5, respectively. Completion of weight adaptation for the 13 data pairs of all the five training sets constitutes one iteration. For effective learning, $100,000$ iterations were made to train the MLP model. To improve learning of the MLP, the learning parameter used in the BP algorithm was varied as:

$$\alpha_i = \alpha_{i-1}(1 - i/N_t), \tag{11}$$

where i is the current iteration number and N_t is the total number of iterations used. Using a Pentium 4, 2.8 GHz machine, it took only 16 seconds to train the MLP with $100,000$ iterations. At the end, the final weights (W) of the MLP were saved for performance evaluation and actual use of the model.

The convergence characteristics of the MLP for the different nonlinear dependencies are shown in Fig. 6. It can be seen that the mean square error (MSE) reaches at about -50 dB within 1000 iterations. However, for better learning, we continued training up to 100,000 iterations.

Performance evaluation of the MLP-based sensor model was carried out by loading the final stored weights into the MLP. It may be noted that, during testing, and actual use of the CPS model, updating of the weights does not take place. After loading the saved weights into the MLP, when the inputs are applied to the MLP model, it estimates the pressure readout. The estimated pressure and the actual applied pressure were compared to find the effectiveness of the model.

VI. RESULTS AND DISCUSSIONS

Based on the results of the simulation study, we provide here the performance evaluation of the MLP-based model for linearization and auto-compensation for the CPS. In addition, we have provided the performance results of an ELM-based CPS model.

A. Linear Response Characteristics

The MLP-based model was found to be capable of producing linear response characteristics. The results obtained through the simulation for the linear and three forms of nonlinear temperature dependencies are provided in Fig. 7. The response characteristics at different temperatures ($-40, 100, 150$ and 200^0C) for $NL0$, $NL1$ and $NL3$ are perfectly linear. However, in the case of $NL2$, for lower ranges of P_N, there is a slight deviation from linearity. The upper curve

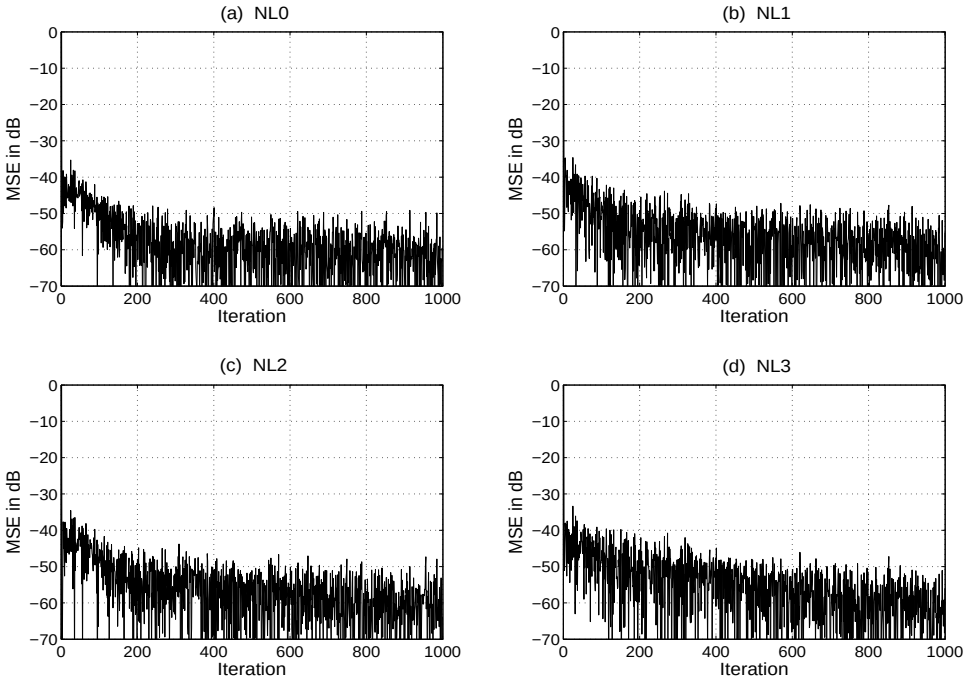

Fig. 6. The convergence characteristics of the MLP for the four temperature dependencies. (a) $NL0$; (b) $NL1$; (c) $NL2$; (d) $NL3$.

which represents the sensor characteristics (SCI output) at the reference temperature ($T_0 = 25^0C$), is shown for the purpose of comparison.

It may be noted that, during training phase, the MLP was not trained with the sensor characteristics for the temperature values in the test set. It may be observed from these figures that the MLP is able to transfer SCI output voltage from the actual to the linearized values quite effectively over a wide range of temperature and for the linear as well as the three forms of nonlinear dependencies. Moreover, it is true even for the unseen situations for which it was not trained.

B. Full Scale Error

The full-scale percent error is used as a performance criterion in this study. It is given by:

$$FS = [P_{Ntru} - P_{Nest}] \times 100, \tag{12}$$

where, the true normalized pressure and estimated normalized pressure are denoted by P_{Ntru} and P_{Nest}, respectively. Here the full scale is assumed to be 1.0. The FS percent error in estimation of normalized response at different temperatures for the $NL0$, $NL1$, $NL2$ and $NL3$ are plotted in Fig. 8. It may be seen that the FS error remains within $\pm 0.5\%$ for a wide range of temperature from -50^0C to 200^0C (at the specified P_N values) for $NL0$, $NL1$, and $NL3$. However, for $NL2$, the FS error varies between -0.75% to 1.5%.

The FS error between the estimated and desired responses at specific values of temperature are shown in Fig. 9. From Fig. 8 and Fig. 9 one can see that the maximum FS error remains within $\pm 0.5\%$ for the $NL0$ and $NL1$. The FS error for $NL2$ remains between -0.75 and 1.5%, and for $NL3$, it varies between $\pm 0.75\%$.

The performance of the CPS linearization using an ELM is carried out. In this case, we used 10 hidden nodes with sigmoid nonlinearity. We have observed that increasing the number of hidden nodes does not improve the performance. The FS percent error and the estimated output obtained from an ELM-based model are shown in Fig. 10 and Fig. 11, respectively. It is seen that the FS error in the ELM-based model is slightly higher and its linearization is slightly inferior to that of the MLP-based model. This may be due to the fact that the selection of the input-layer random weight matrix might not be a proper one.

The most important benefit of using ELM is its extremely low computation time. The ELM-based CPS model took only a fraction of second to train. Thus, it has a great advantage over MLP-based model, as the latter took about 16 seconds to train for 100,000 iterations. For this reason, the ELM-based model may be used for on-line applications. In addition to ELM, other NN architectures, for example, RBF and Bayesian NNs may be studied. We believe that these NNs will provide satisfactory performance results at higher computational cost.

VII. EXPERIMENTAL SETUP AND RESULTS

In order to demonstrate the effectiveness of MLP-based model on real sensor data, we collected data from a force sensor with an experimental setup. In this section we briefly describe the setup and show the necessary results.

A. Experimental Setup

The experimental setup to obtain sensor output at different temperatures is shown in Fig. 12. We used a Celoxica RC203E Development Board with Xilinx Virtex-II FPGA chip to obtain digital readouts. A Honeywell FSG15N1A force sensor is used to measure the applied weight and National Semiconductor

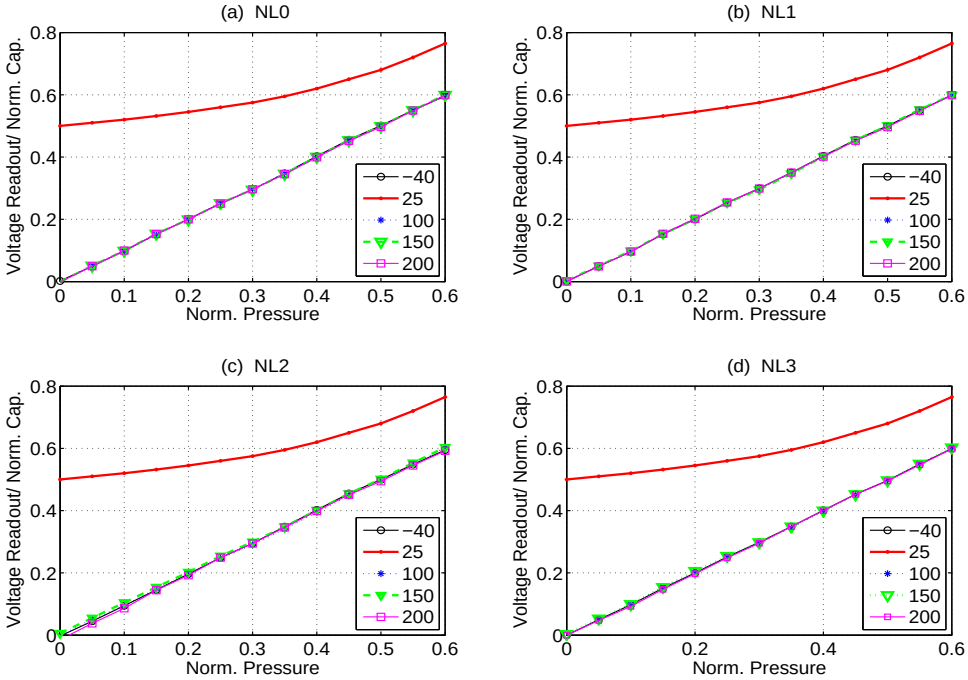

Fig. 7. Linearized response characteristics achieved by the MLP-based model. The response characteristics shown are for different temperatures ($-40, 25, 100, 150$ and 200^0C) of the *test set* for a linear and three forms of nonlinear dependencies. (a) $NL0$; (b) $NL1$; (c) $NL2$; (d) $NL3$.

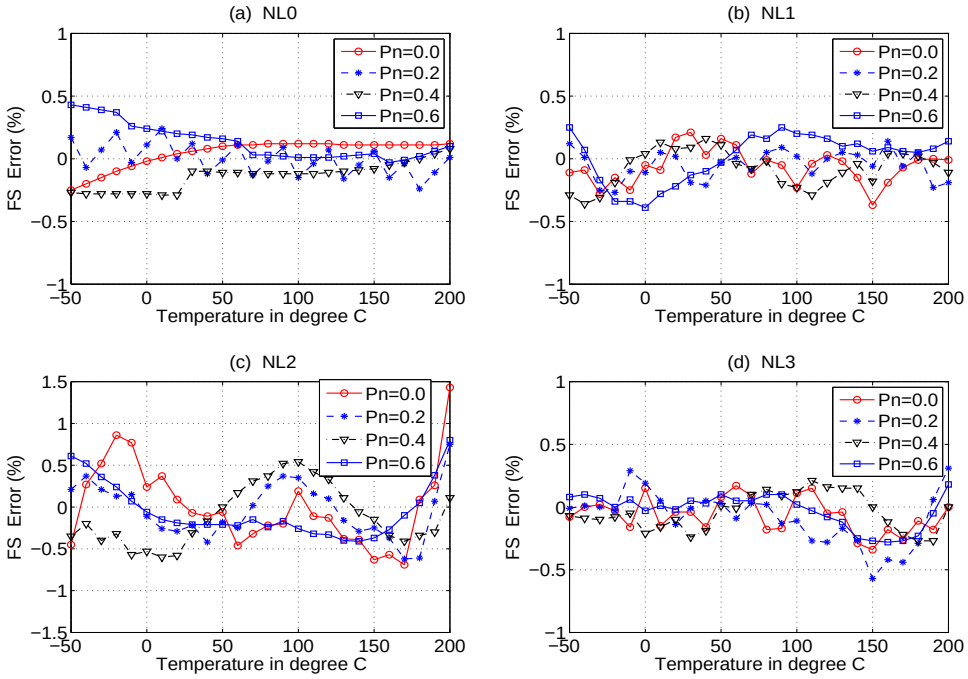

Fig. 8. Full-scale percent error between the linearized and estimated responses at different values of P_N ($P_N = 0.0, 0.2, 0.4$ and 0.6) for a linear and three forms of nonlinear dependencies. (a) $NL0$; (b) $NL1$; (c) $NL2$; (d) $NL3$.

LM35CZ temperature sensor was used to measure the environmental temperature. A mechanical platform was fabricated to mount different weights on the force sensor. The force sensor and temperature sensor outputs were amplified and then applied to a multiplexer (MUX). The MUX output was passed through a sample-and hold (S/H) circuit and then converted into digital form by a 12-bit analog to digital converter (ADC). The digital readout of the applied weight and environmental temperature were recorded using the RC203E development board. We used an electric oven to control the surrounding temperature.

We applied weights to the force sensor's mechanical platform at an increment of 20 grams to obtain digital readout for 0-500 grams, at five different temperatures, i.e., at 12, 22, 40, 60 and 80^0C. To minimize the effect of measurement noise, the measured data were averaged over several experiments.

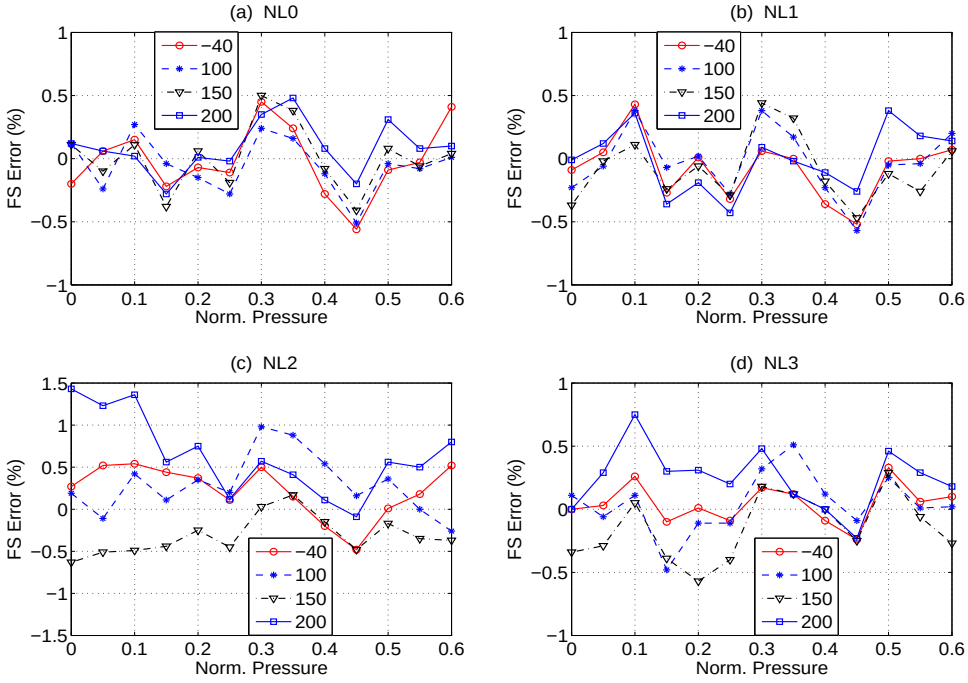

Fig. 9. Full-scale percent error between the linearized and estimated responses at specific temperatures (-40, 100, 150 and 200^0C) for a linear and three forms of nonlinear dependencies: (a) $NL0$; (b) $NL1$; (c) $NL2$; (d) $NL3$.

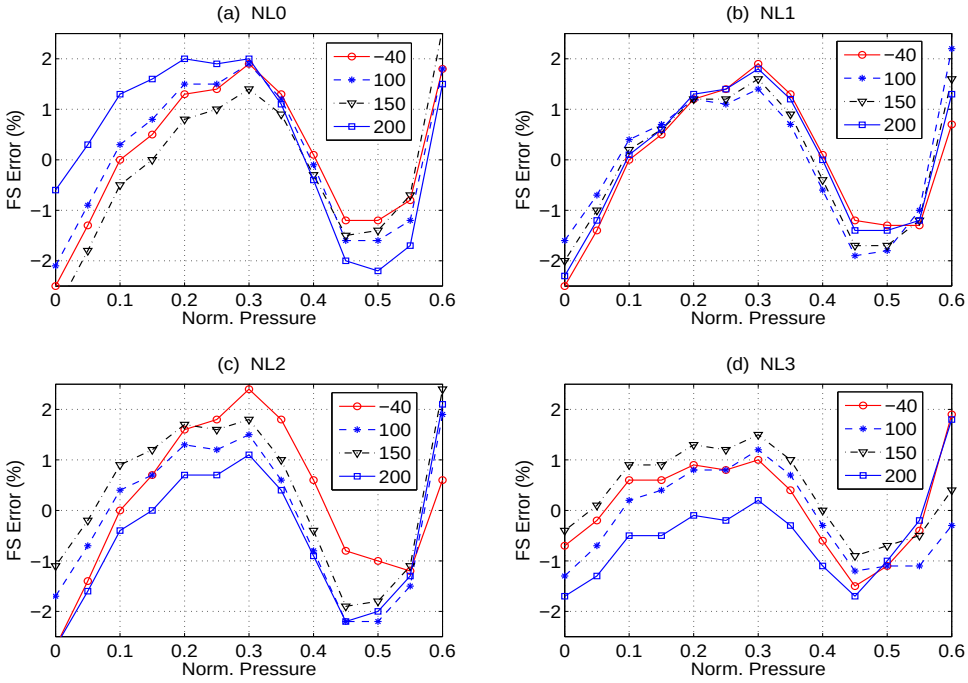

Fig. 10. Performance of ELM-based model. Full-scale percent error between the linearized and estimated responses at specific temperatures (-40, 100, 150 and 200^0C) for a linear and three forms of nonlinear dependencies: (a) $NL0$; (b) $NL1$; (c) $NL2$; (d) $NL3$.

The measured digital readout (in mv) against input weights (in grams) at five different temperatures are shown in Fig. 13 (upper five dotted lines). It can be seen that the response of the force sensor is nonlinear and dependent on the environmental temperature.

B. Experimental Results

An MLP with $\{2-5-1\}$ architecture was selected for modeling the force sensor. The MLP was trained with three datasets (at $12, 40$ and 80^0C) for $20,000$ iterations using learning and momentum factors as 0.05 and 0.25, respectively. During training we used only five data points (out of 26 data points) from each data set. The lower curves in Fig. 13 represent the estimated response by the MLP-based model. It

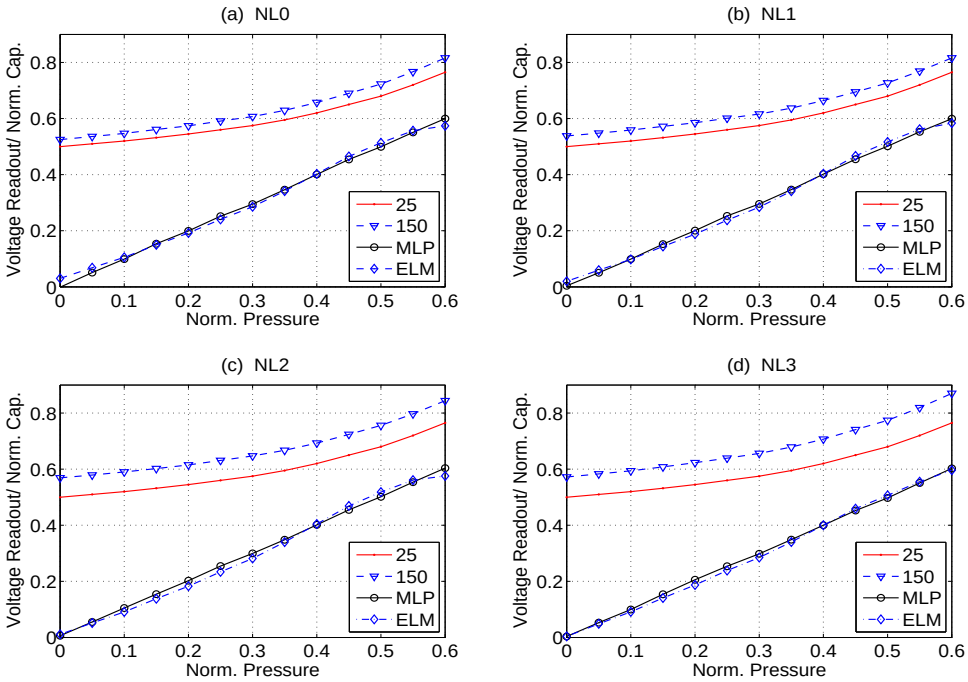

Fig. 11. Performance comparison between the MLP- and ELM-based sensor models at 150^0C. The actual CPS response at 25^0C is also shown for comparison. (a) $NL0$; (b) $NL1$; (c) $NL2$; (d) $NL3$.

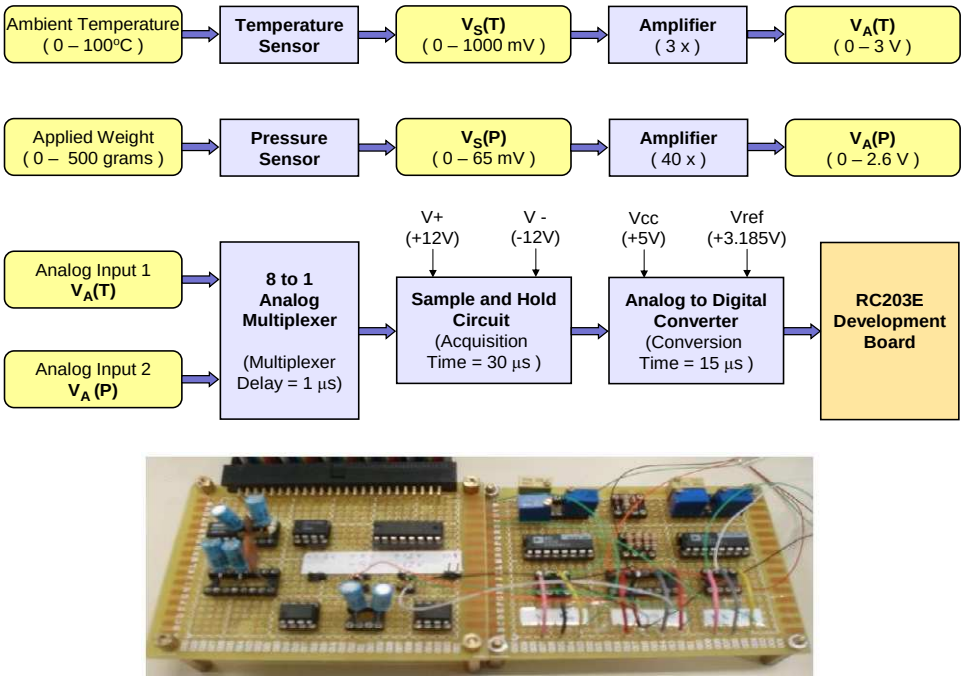

Fig. 12. Schematic of the experimental setup.

can be seen that the MLP-based model output is almost linear.

The FS error between the linearized response and the actual response from the MLP-based model is depicted in Fig. 14. The FS error is about $\pm 1.5\%$. The relatively higher FS error is due to the presence of noise in the data used to train the MLP. However, even with these noisy data, performance of the MLP-based model is found to be satisfactory and the FS error remains within $\pm 1.5\%$.

VIII. CONCLUSIONS

Smart sensors should be capable of providing accurate readout, calibration and auto-compensation for the nonlinear influences of the environmental parameters on its characteristics. To achieve these objectives, we have proposed a novel neural network-based technique for modeling a capacitive pressure sensor operating in a harsh environment in which temperature can have wide range of variation. Using a variable learning

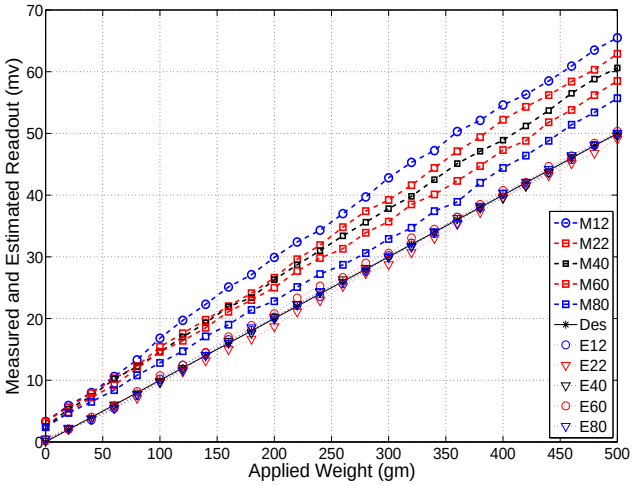

Fig. 13. The measured force sensor characteristics (upper five curves). The bottom curves correspond to the estimated linearized response by the MLP model. In the legend 'M**' and 'E**' represent the measured and estimated values, respectively.

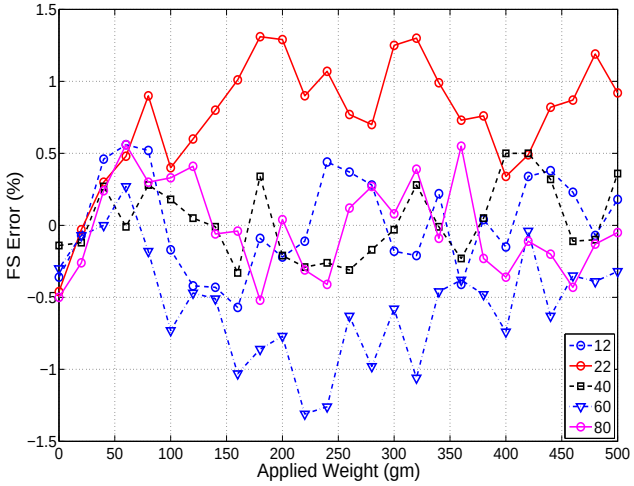

Fig. 14. The FS error between desired linearized characteristics and MLP-model's output.

rate backpropagation algorithm and taking random samples during training, a highly effective NN-based CPS model was obtained. We have shown the effectiveness of the proposed model under different forms of nonlinear influences of the ambient temperature on the pressure sensor characteristics.

We have considered a linear form and three forms of nonlinear influences of temperature on the sensor characteristics in a temperature range varying from -50 to 200^0C. The maximum error of the NN model for estimation of pressure remains within $\pm 1.0\%$ (FS) for the linear form, while it remains within $\pm 1.5\%$ for the three forms of nonlinear dependencies. The proposed NN-based models may be applied to other types of sensors to incorporate intelligence in terms of auto-calibration and to mitigate the nonlinear dependency of their response characteristics on the environmental parameters.

We have compared the performance of the MLP-based CPS model with another highly efficient and powerful NN, /it i.e. , ELM. Performance of the ELM-based CPS model is found to be slightly inferior to that of the MLP-based model. However, ELM is found to be computationally more efficient and therefore may be used for on-line applications. The performance of the MLP-based model based on the measured data obtained through an experimental setup is also found to be satisfactory. We believe that other NN models, *e.g.* , RBF and Bayesian NNs, may also provide satisfactory performance in similar applications.

REFERENCES

[1] F. M. L. van der Goes and G. C. M. Meijer, "A simple accurate bridge-transducer interface with continuous autocalibration," *IEEE Trans. Instrum. and Meas.*, vol. 46, no. 3, pp. 704-710, June 1997.

[2] X. Li and G. C. Meijer, "An accurate interface for capacitive sensors," *IEEE Trans. Instrum. and Meas.*, vol. 51, no.5, pp. 935-939, Oct. 2002.

[3] M. Yamada, T. Takebayashi, S-I. Notoyama, and K. Watanabe, "A switched-capacitor interface for capacitive pressure sensors," *IEEE Trans. Instrum. and Meas.*, vol. 41, no. 1, pp. 81-86, Feb. 1992.

[4] M. Yamada and K. Watanabe, "A capacitive pressure sensor interface using oversampling $\Delta - \Sigma$ demodulation techniques,", *IEEE Trans. Instrum. and Meas.*, vol. 46, no. 1, pp. 3-7, Feb. 1997.

[5] P. Hille, R. Hohler, and H. Strack, "A linearization and compensation method for integrated sensors," *Sensors and Actuators-B*, vol. 44, pp. 95-102, 1994.

[6] A. M. Sabatini, "A digital signal-processing technique for compensating ultrasonic sensors," *IEEE Trans. Instrum. and Meas.*, vol. 46, no. 4, pp. 869-874, Aug. 1995.

[7] I. Maric, "Automatic digital correction of measurement data based on M-point autocalibration and inverse polynomial approximation," IEEE Trans. Industrial Electronics, vol. 35, no. 2, pp. 317-322, May 1988.

[8] K. F. Lyahou, G. van der Horn, and J. H. Huijsing, "A noniterative polynomial 2-D calibration method implemented in a microcontroller," *IEEE Trans. Instrum. and Meas.*, vol. 46, no. 4, pp. 752-757, Aug. 1997.

[9] X. Li, G. C. Meijer, G. W. de Jong, "A microcontroller-based self-calibration technique for a smart capacitance angular-position sensor," *IEEE Trans. Instrum. and Meas.*, vol. 46, no.4, pp. 888-892, Aug. 1997.

[10] X. Li, M. Bao and S. Shen, "Study on linearization of capacitive pressure sensors," *Sensors and Actuators A*, vol. 63, pp. 1-6, 1997.

[11] S. Poussier, H. Rabah and S. Weber, "Adaptable thermal compensation system for strain gause sensors based on programmable chip," *Sensors and Actuators A*, vol. 119, pp. 412-417, 2005.

[12] J. M. Dias Pereira, O. Postolache and P. Silva Girao, "Adaptive self-calibration algorithm for smart sensors linearization," in Proc. *IEEE Intrumentation and Measurement Technology Conrefence* (IMTC 2005), Ottawa, Canada, May 2005.

[13] S. Haykin, *Neural Networks*, Maxwell MacMillan, Ontario, Canada, 1994.

[14] L. F. Pau, F. S. Johansen, "Neural network signal understanding for instrumentation," *IEEE Trans. Instrum. and Meas.*, vol. 39, no.4, pp. 558-564, Aug. 1990.

[15] P. Daponte, D. Grimaldi, "Artificial neural networks in measurements," *Measurement*, vol. 23, pp. 93-115, 1998.

[16] J. M. Dias Pereira, P. M. B. Silva Girao, and O. Postolache, "Fitting transducer characteristics to measured data," *IEEE Instrumentation and Measurement Magazine*, pp. 26-39, Dec. 2001.

[17] R. Z. Morawski, "Digital signal processing in measurement microsystems," *IEEE Instrumentation and Measurement Magazine*, pp. 43-50, June 2004.

[18] A. P. Singh, S. Kumar and T. S. Kamal, "Fitting transducer characteristics to measured data using a virtual curve tracer," *Sensors and Actuators-A*, vol. 111, pp. 145-153, 2004.

[19] J. C. Patra, A. C. Kot, and G. Panda, "An intelligent pressure sensor using neural networks," *IEEE Trans. Instrum. and Meas.*, vol. 49, no. 4, pp. 829-834, Aug. 2000.

[20] J. C. Patra, A. van den Bos, and A. C. Kot, "An NN-based smart capacitive pressure sensor in dynamic environment," *Sensors and Actuators-B*, vol. 86, pp. 26-38, 2000.

[21] J. C. Patra, E. L. Ang, N. S. Chaudhari and A. Das, "Neural- network-based smart sensor framework operating in a harsh environment," *Journal of Applied Signal Processing*, vol. 4, pp. 558-574, 2005.

[22] J. M. Dias Pereira, O. Postolache, and P. M. B. Girao, ”A temperature compensated system for magnetic field measurements based on artificial neural networks,” *IEEE Trans. Instrum. and Meas.*, vol. 47, no. 2, pp. 494-498, Apr. 1998.

[23] A. Carullo, F. Ferraris, S. Graziani, U. Grimaldi, and M. Parvis, ”Ultrasonic distance sensor improvement using a two-level neural networks,” *IEEE Trans. Instrum. and Meas.*, vol. 45, pp. 677-682, Apr. 1996.

[24] P. Arpaia, P. Daponte, D. Grimaldi, and L. Michaeli, ”ANN-based error reduction for experimentally modeled sensors,” *IEEE Trans. Instrum. and Meas.*, vol. 51, no. 1, pp. 23-30, Feb. 2002.

[25] A. P. Singh, S. Kumar and T. S. Kamal, ”Development of ANN-based virtual fault detector for Wheatstone bridge-oriented transducer,” *IEEE Sensors Journal*, vol. 5, pp. 1043-1049, Oct. 2005.

[26] A. P. Singh, S. Kumar and T. S. Kamal, ”Virtual compensator for correcting the disturbing variable effect in transducers,” *Sensors and Actuators-A*, vol. 116, pp. 1-9, 2004.

[27] N. J. Medrano-Marques and B. Martin-del-Brio, ”Sensor linearization with neural networks,” *IEEE Trans. Industrial Electronics*, vol. 48, no. 6, pp. 1288-1290, Dec. 2001.

[28] G. -B. Huang, Q.-Y. Zhu and C.-K. Siew, Extreme learning machine: theory and applications, *Neurocomputing*, vol. 70, pp. 489-501, 2006.

[29] G. -B. Huang, Q. -Y. Zhu, and C. -K. Siew, ”Real-time learning capability of neural networks,” *IEEE Trans. Neural Networks*, vol. 17, no. 4, pp. 863-878, July 2006.

[30] G. -B. Huang, L. Chen and C. -K. Siew, ”Universal approximation using incremental constructive feedforward networks with random hidden nodes,” *IEEE Trans. Neural Networks*, vol. 17, no. 4, pp. 879-892, July 2006.

[31] N. -Y. Liang, G. -B. Huang, P. Saratchandran and N. Sundararajan, ”A fast and accurate online sequential learning algorithm for feedforward networks,” *IEEE Trans. Neural Networks*, vol. 17, no. 6, pp. 1141-1423, Nov. 2006.